[15]J. W. Butler, "A proposed electromagnetic momentum-energy 4-vector for charged bodies," Am. J. Phys. **37**, 1258–1272 (1969).
[16]F. Rohrlich, "Comment on the preceding paper by T. H. Boyer," Phys. Rev. D **25**, 3251–3255 (1982).
[17]T. H. Boyer, "Classical model of the electron and the definition of electromagnetic field momentum," Phys. Rev. D **25**, 3246–3250 (1982).
[18]F. Rohrlich, "Self-energy and stability of the classical electron," Am. J. Phys. **28**, 639–643 (1960).

Teaching physics with 670-nm diode lasers—experiments with Fabry–Perot cavities

R. A. Boyd, J. L. Bliss, and K. G. Libbrecht[a)]
Norman Bridge Laboratory of Physics, California Institute of Technology 12-33, Pasadena, California 91125

(Received 19 February 1996; accepted 9 May 1996)

In a previous paper we described details of the construction of stabilized 670-nm diode lasers for use in undergraduate physics laboratories. We report here a series of experiments that can be performed using the 670-nm diode laser, a homemade scanning Fabry–Perot cavity, a helium–neon laser, a simple photodiode, and a few pieces of electronics hardware. The experiments include: (1) an introduction to the scanning confocal Fabry–Perot cavity, and to its use as an optical spectrum analyzer; (2) laser frequency modulation and observation of FM sidebands using the optical spectrum analyzer; and (3) the Pound–Drever method for servo-locking a Fabry–Perot cavity to a laser. These experiments are relatively easy to set up and perform, yet they demonstrate a number of useful optical principles and experimental techniques. © *1996 American Association of Physics Teachers.*

I. INTRODUCTION

In a previous paper by Libbrecht *et al.*[1] we described the construction of stabilized 670-nm semiconductor diode lasers for use in undergraduate teaching laboratories. These inexpensive visible lasers emit tunable coherent light which can be used to perform a number of interesting and fundamental physics experiments. The lasers provide the foundation for a new 9-week (one quarter) senior physics lab course at Caltech, which consists of a series of experiments in optical and atomic physics.

An attractive feature of the Caltech course is that it is track based, i.e., students all follow the same track in parallel. The course begins with simpler experiments to build up experience with the equipment and the physics; students then move on to more complex experiments as the course progresses. The equipment needed for these experiments is sufficiently inexpensive that several setups can operate simultaneously, which is necessary for a track-based course.[2]

We describe here a series of three experiments involving lasers and Fabry–Perot cavities. The first (and simplest) experiment consists of aligning two spherical mirrors to form a confocal cavity, and using the cavity as an optical spectrum analyzer. This familiarizes the students with basic Fabry–Perot cavity concepts and gives them experience aligning an optical cavity.

In the second experiment, the students use their optical spectrum analyzer to observe FM sidebands on a diode laser beam. The sidebands are produced by rf modulation of the diode's injection current. The shape of the FM sidebands is readily calculated, and students have the opportunity to compare their calculated spectra with observed spectra.

In the third experiment, the students use the Pound–Drever method to lock a Fabry–Perot resonance frequency to the diode laser's frequency. FM sidebands are added to the optical carrier, and an optical rf circuit produces an electronic error signal which is related to the difference between the laser frequency and the resonance frequency of the nearest longitudinal cavity mode. The error signal is then used to servo-lock the cavity to the laser. In our experience this experiment is particularly popular. It involves concepts that are both powerful and fairly easy to grasp, and most of our undergraduate students (physics majors) are unfamiliar with rf technology and servo mechanisms at the beginning of the course.

The first of these three experiments is not unlike other undergraduate laboratory experiments involving Fabry–Perot cavities.[3–6] The other two experiments, however, since they require the addition of rf sidebands to the laser, are usually considered too expensive for a teaching lab. This is no longer the case, since sidebands can be easily added to a diode laser's output via rf modulation of the laser's injection current, as is described below.

II. THE OPTICAL SPECTRUM ANALYZER

Fabry–Perot cavities are in widespread use in optical physics, for such applications as sensitive wavelength discriminators and for building up large light intensities from modest input powers. In this first experiment students assemble a Fabry–Perot cavity and examine its properties. Figure 1 shows the basic Fabry–Perot cavity, consisting of two spherical mirrors separated by a distance L. An excellent detailed discussion of the properties of Fabry–Perot cavities is given by Yariv.[7]

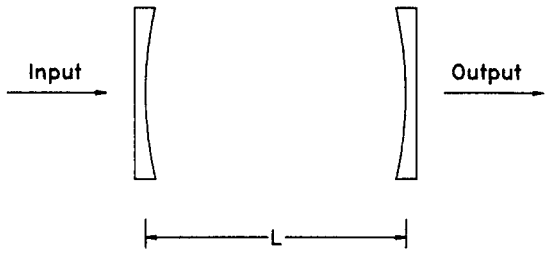

Fig. 1. The basic Fabry–Perot cavity. The spherical surfaces of the mirrors are coated for high reflectivity, while the flat surfaces are antireflection coated and have negligible reflectivity.

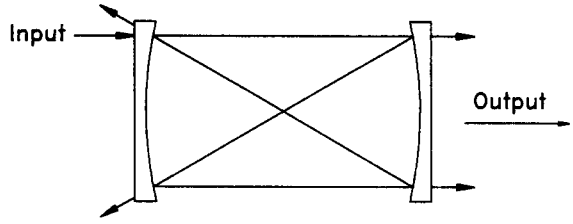

Fig. 3. Ray paths for a slightly misaligned confocal Fabry–Perot cavity (the off-axis scale is exaggerated). Note the two backreflected beams are not coincident in direction with the input beam, and thus are less apt to create serious problems with diode laser feedback.

To briefly review the basics, consider two identical plane mirrors, each with reflectivity R and transmission T ($R+T=1$), separated by a distance L. This etalon has transmission peaks at frequencies $\nu_m = mc/2nL$, where m is an integer, c is the speed of light, and n is the index of refraction inside the etalon (which we take here to be unity). The separation between two peaks, called the "free-spectral range," is given by

$$\Delta\nu_{\mathrm{FSR}} = c/2L.$$

If the mirror reflectivity is high (for our mirrors it is approximately 99.5% at 671 nm), then the transmission peaks will be narrow compared with $\Delta\nu_{\mathrm{FSR}}$. The full width at half maximum $\Delta\nu_{\mathrm{FWHM}}$ of the peaks is given by

$$\Delta\nu_{\mathrm{FWHM}} = \Delta\nu_{\mathrm{FSR}}/F,$$

where $F = \pi\sqrt{R}/(1-R)$ is called the cavity "finesse." If there is scattering or absorption in the cavity or mirrors, then the peak transmission is

$$\frac{4T^2}{(2T+\epsilon)^2},$$

where ϵ equals the round-trip fractional loss in the cavity.

A Fabry–Perot cavity can be considered both as an interferometer and as an optical resonator. If the input laser frequency is not near ν_m, the beam effectively reflects off the first mirror (which has a high reflectivity). If, however, the input frequency is equal to ν_m, then light in the cavity destructively interferes with the reflected beam. Immediately after the input laser beam is turned on, the power inside the cavity builds up until the light leaking out of the cavity back toward the laser exactly cancels the reflected input beam. The intensity of the transmitted beam then equals the intensity of the input beam (neglecting cavity losses). Hence, at ν_m the total cavity transmission is unity, and the intensity inside the cavity is $\approx 1/T$ times as large as that of the input beam.

To make an optical spectrum analyzer, the length of the cavity must be scanned. We accomplish this by attaching one mirror to a piezoelectric tube (PZT), as is shown in Fig. 2. Applying a triangle-wave voltage to the PZT scans the spacing L a small amount, thus scanning the peak frequencies ν_m. If the laser beam contains frequencies in a range around some ν_0, then by scanning the PZT one can record the laser spectrum, as shown schematically in Fig. 2. Note that there is some ambiguity in the spectrum; a laser with two modes at frequencies ν_0 and $\nu_0+\delta\nu$ would produce a spectrum identical to that of a laser with modes at ν_0 and $\nu_0+\delta\nu+j\Delta\nu_{\mathrm{FSR}}$, where j is any integer.

The above simple picture does not quite correspond with reality because only the *longitudinal* modes of the Fabry–

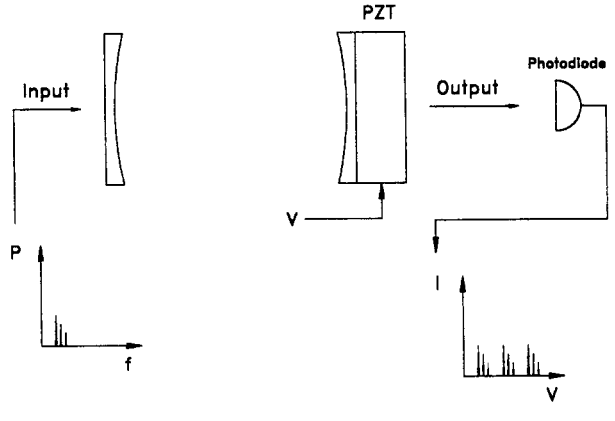

Fig. 2. Using a Fabry–Perot cavity as an optical spectrum analyzer. Here the input laser power as a function of frequency $P(f)$ is shown with a multimode structure. By scanning the cavity length with a PZT tube, the laser's mode structure can be seen in the photodiode output as a function of PZT voltage $I(V)$. Note that the signal repeats with the period of the cavity free-spectral range.

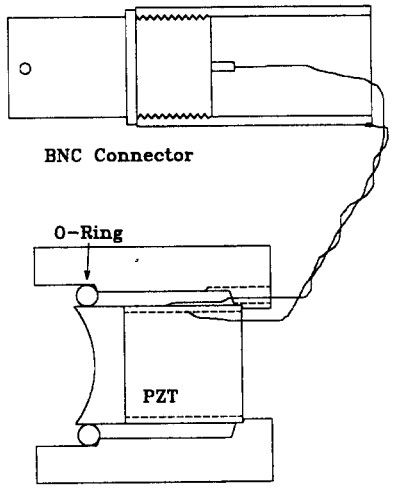

Fig. 4. Mechanical mounting details for the Fabry–Perot mirror and PZT. The mirror and PZT tube are mounted inside a 1-in-diam aluminum housing, which can itself be mounted in a larger (1-in. i.d.) tube or any standard 1-in. mirror mount. The $\frac{1}{2}$-in. copper tube containing the BNC connector can be mounted in a right-angle post-clamp for strain relief.

Perot cavity have been considered. In addition to these modes, an infinite number of *transverse* modes can resonate within the cavity; the frequencies of the transverse modes are, in general, different from ν_m. Examples of low-order transverse modes in an optical resonator are shown in Fig. 2-8 of Yariv.[7] Very-high-order transverse modes are not important, since their extent in the transverse direction is so great that they do not hit the small cavity mirrors. Also, a nearly-on-axis laser will preferentially excite the low-order modes. For a random cavity length L, these low-order transverse modes greatly complicate the simple picture shown in Fig. 2.

It is possible (using a properly placed lens) to "mode-match" the Gaussian mode of the laser with the TM_{00} mode of the cavity; then one observes only the longitudinal modes as the cavity length is scanned. However, the optical feedback from a mode-matched cavity is sufficient to destabilize almost any diode laser's operation, and an optical isolator is needed to get good results.

However, if we choose the cavity length to be equal to the radius of curvature of the Fabry–Perot mirrors, then the low-order transverse modes become degenerate in frequency, with a separation $c/4L=\Delta\nu_{FSR}/2$ (see Yariv,[7] Sec. 4.6). For this special case, called a "confocal" cavity, the spectrum will look just like that of Fig. 2, except with a mode spacing $\Delta\nu_{confocal}=c/4L$. Another nice feature of the confocal cavity is that the cavity transmission is insensitive to the laser alignment, as shown in Fig. 3. This allows an intentional slight misalignment of the input beam, preventing a strong backreflection which could upset the diode laser operation.

To realize a simple Fabry–Perot cavity in the lab, we use mirrors which were specially made for this purpose.[8] Our mirrors are $\frac{1}{2}$-in.-diam spherical mirrors with a 20-cm radius of curvature. The flat side is antireflection coated for 671 nm (the wavelength of our diode lasers), and the curved side is coated for 0.5% transmission at 671 nm. Losses in the mirrors are typically less than 0.25%. By accident (although this could be specified) the reflectivity of our mirrors at 633 nm (the He–Ne laser wavelength) is very high. These mirrors are unfortunately quite expensive in small quantities, since special coating runs are necessary. Since many (20 or more) mirrors can be coated simultaneously, it is advantageous to order in large quantities and to split the order with others, if possible.

The mirror/PZT assembly is shown in Fig. 4. To put the assembly together, one first solders leads to the PZT tube, which, in our case, is the same type of PZT as those in our stabilized diode lasers.[1] One then epoxies the mirror to the PZT tube, being careful to apply epoxy only around the mirror edge. Only a small amount of epoxy is needed for this step, since stresses on the final assembly are small. Five-minute epoxy works well for this purpose. The mirror/PZT is then placed in the aluminum housing shown in Fig. 4 and held in place with an O-ring. The PZT tube is glued to the aluminum tube by applying a small bead of epoxy around the inside of the PZT tube. Note that the mirror is free to move as the PZT tube expands and contracts. The PZT leads are soldered to a BNC connector, which is screwed into a short piece of $\frac{1}{2}$-in.-diam copper tubing. The tubing serves to enclose the high-voltage pin of the BNC. The BNC assembly can then be mounted using a right-angle post-clamp[9] to the mounting post that supports the Fabry–Perot cavity, providing necessary strain relief. The mirror/PZT assembly can be mounted in any standard 1-in. mirror mount, or inside a "cavity tube" with a 1-in. i.d., which forms the Fabry–Perot cavity. We have found that the latter makes a much more stable cavity. The opposite mirror is mounted in a $\frac{1}{2}$-in. to 1-in. adapter,[10] which is then placed in the other end of the cavity tube. The PZT tube is driven using the same high-voltage controller normally used for the diode laser.[1] Note that the experiments described here do not require precise tuning of the laser frequency; hence, one does not need an additional high-voltage controller for the laser.

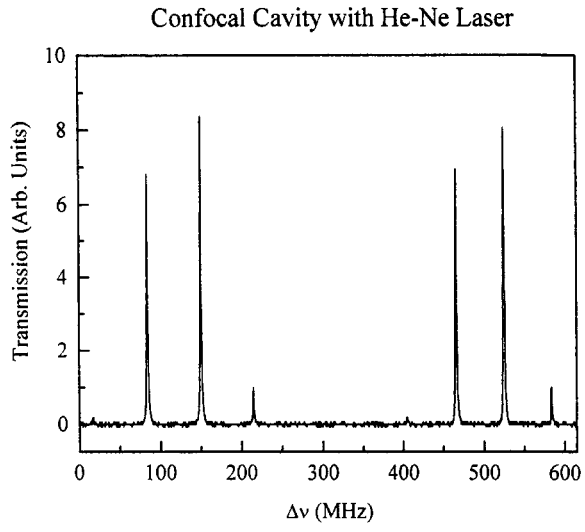

Fig. 5. Measured cavity transmission as a function of PZT voltage, where here the voltage has been normalized to cavity frequency. The input beam was a multimode He–Ne laser. Note the repetition of the spectrum with a spacing equal to the confocal free-spectral-range $\Delta\nu_{confocal}=c/4L=375$ MHz.

The purpose of this lab is to understand the basic principles of Fabry–Perot cavities and to examine some of their properties. A first exercise is to set up the cavity with a random mirror spacing ($\neq$20 cm), and to examine the cavity transmission using an He–Ne laser as the cavity spacing is scanned (see Fig. 2). One observes a jumble of sharp peaks that are very sensitive to the alignment of the cavity. These peaks are some of the various longitudinal and transverse modes of the cavity.

The next exercise is to set the mirror spacing to 20 cm, the confocal spacing, and to use the cavity as an optical spectrum analyzer. Figure 5 shows a typical spectrum obtained in this manner, using an He–Ne laser that runs in several modes simultaneously. These data were acquired using a versatile digital storage oscilloscope,[11] and then transferred via a GPIB cable to a personal computer for display. The length of the He–Ne laser cavity can be determined (with some ambiguity) from the spacing of the peaks in this figure.

Figure 6 shows a portion of the same spectrum as in Fig. 5, but with the mirror spacing changed slightly from the confocal spacing. Note the emergence of many almost-degenerate transverse modes in the spectrum. Note also that the confocal peaks in Fig. 6(a) have larger widths than the peaks in Fig. 6(c); furthermore, a calculation based on the measured reflectivity of the mirrors gives a significantly narrower linewidth than that measured from Fig. 6(a). This shows that the linewidth of the confocal peaks is determined mainly by imperfect cavity alignment, and not by the intrinsic reflectivity of the cavity mirrors.

In order to make a quantitative comparison of the confocal

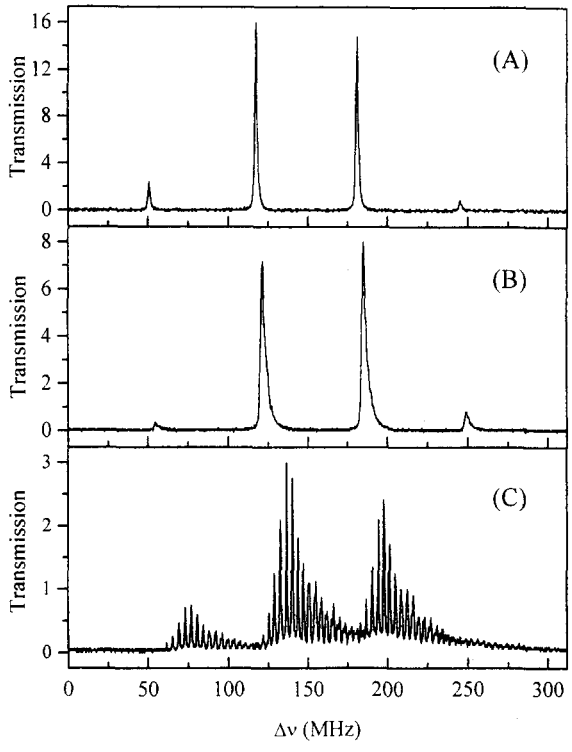

Fig. 6. A close-up of the spectrum in Fig. 5. In (A) the cavity length was adjusted to be as close as possible to the confocal length, giving narrow symmetric lines. In (B) and (C) the length was made progressively further from the confocal length, giving asymmetric lines in (B), and showing many transverse cavity modes in (C). Note the height of the peaks diminishes as the power is spread over a larger frequency range.

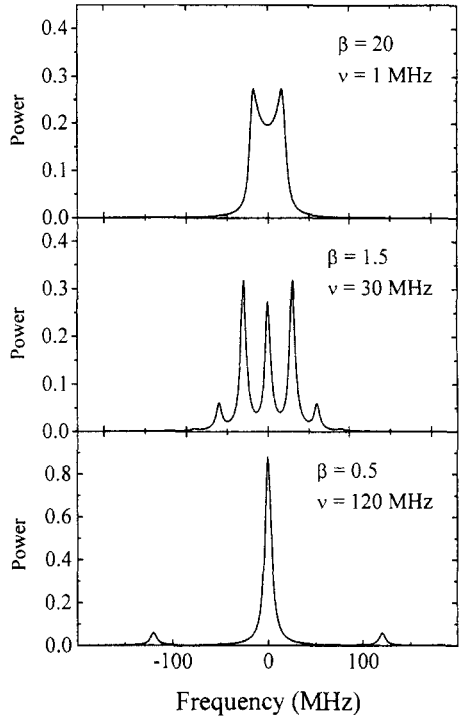

Fig. 7. Calculated FM spectra as described in the text, with different values of the modulation frequency $\nu=\Omega/2\pi$ and modulation index β, as marked.

cavity transmission spectrum with a calculated one, we place a beamsplitter (a small piece of microscope slide works nicely) inside the cavity tube through a slot in its side. Light reflecting off the beamsplitter is then lost from the cavity. The spectrum of the modified cavity is essentially the same as a plain cavity, except with a lower effective mirror reflectivity. (A detailed calculation of the cavity transmission is a straightforward exercise for the student.) The transmission peaks of the modified cavity are typically so broad that slight imperfections in the cavity alignment have little effect on the measured spectrum. By separately measuring the single-pass loss from the beamsplitter, one is then able to compare measured and calculated cavity transmission spectra.

III. FREQUENCY-MODULATION SPECTROSCOPY

In the radio-frequency domain there exists a substantial technology devoted to amplitude modulation (AM) and frequency modulation (FM) of an electromagnetic carrier wave. If one boosts the carrier frequency from 100 MHz (typical of FM radio) to around 500 THz (optical), the same ideas apply to AM and FM modulation of light. The resulting optical technology has many scientific and engineering applications, the most dominant being in fiber-optic communications.

The light emitted from a semiconductor diode laser is easily modulated by applying a small rf modulation to the injection current.[12] This produces both AM and FM modulation of the optical field, but the former is fairly small and can for the most part be neglected. For pure FM modulation we can write the optical field as

$$\mathbf{E}(t)=\mathbf{E}_0\exp[-i\omega_0 t-i\varphi(t)],$$

where $\varphi(t)$ is the modulated phase of the laser output. We assume that $\varphi(t)$ is slowly varying compared to the unmodulated phase change $\omega_0 t$, since ω_0 is at optical frequencies and the modulation is at radio frequencies. For pure sinusoidal modulation,

$$\varphi(t)=\beta\sin(\Omega t),$$

where Ω is the modulation frequency and β, the modulation index, gives the peak phase excursion induced by the modulation.[13] If we note that the instantaneous optical frequency is given by the instantaneous rate-of-change of the total phase, we have

$$\begin{aligned}\omega_{\text{inst}}&=\omega_0+d\varphi/dt\\&=\omega_0+\beta\Omega\cos(\Omega t)\\&=\omega_0+\Delta\omega\cos(\Omega t),\end{aligned}$$

where $\Delta\omega$ is the maximum frequency excursion. Note that $\beta=\Delta\omega/\Omega$ is equal to the ratio of the maximum frequency excursion to the modulation frequency.

It is useful to expand the above expression for the electric field into a carrier wave and a series of sidebands:[14]

$$\begin{aligned}\mathbf{E}(t)&=\mathbf{E}_0\exp[-i\omega_0 t-i\beta\sin(\Omega t)]\\&=\mathbf{E}_0\sum_{n=-\infty}^{n=\infty}J_n(\beta)\exp[-i(\omega_0+n\Omega)t]\\&=\mathbf{E}_0\Big\{J_0(\beta)\exp(-i\omega_0 t)+\sum_{n=1}^{n=\infty}J_n(\beta)[\exp[-i(\omega_0\\&\quad+n\Omega)t]+(-1)^n\exp[-i(\omega_0-n\Omega)t]]\Big\}.\end{aligned}$$

This transformation shows that the modulated laser field con-

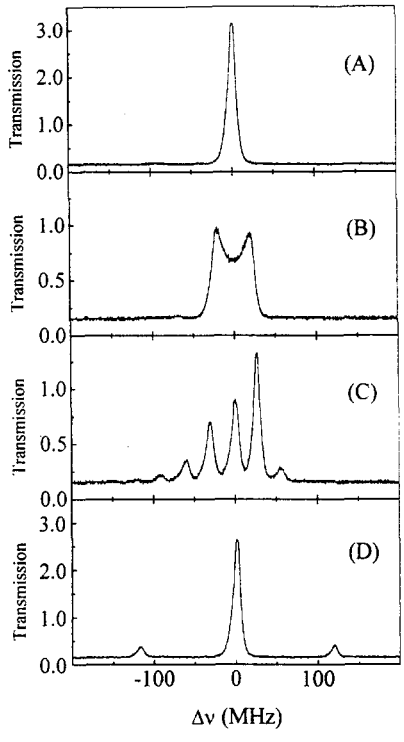

Fig. 8. FM spectra measured using the optical spectrum analyzer described in Sec. II. (A) the unmodulated laser spectrum convolved with the confocal cavity transmission profile; (B) a modulation frequency of $\nu=\Omega/2\pi=1$ MHz and an amplitude of $A=50$ mV (on the rf input of the diode laser current controller); (C) $\nu=30$ MHz and $A=100$ mV; (D) $\nu=120$ MHz and $A=150$ mV. Note the good correspondence with the calculated spectra in Fig. 7, except for the asymmetry in the measured sideband structure caused by residual amplitude modulation of the laser.

sists of a series of spectral features. The J_0 term at the original frequency ω_0 is the optical carrier (in analogy with radio terminology), while the other terms at frequencies $\omega_0 \pm n\Omega$ form sidebands around the carrier. The sideband amplitudes are given by $J_n(\beta)$, which rapidly becomes small for $n>\beta$. Note that the total power in the beam is given by

$$\langle \mathbf{E}\cdot\mathbf{E}^*\rangle = E_0^2\left[J_0^2(\beta)+2\sum_{n=1}^{n=\infty} J_n(\beta)^2\right]=E_0^2,$$

which is independent of β, as it must be for pure frequency modulation. Often one wishes to add two small sidebands around the carrier; for this one wants $\beta \ll 1$, and the sideband power is then given by $\sim J_1(\beta)^2 \approx \beta^2/4$. Evaluating the above sum, and convolving with a Lorentzian laser+cavity spectrum, we have

$$I(\omega)=J_0^2(\beta)L(\omega_0)+\sum_{n=1}^{n=\infty} J_n(\beta)^2[L(\omega_0+n\Omega) + L(\omega_0-n\Omega)],$$

where $L(\omega)$ is a normalized Lorentzian function, which then gives spectra like those shown in Fig. 7. Note that for $\beta \gg 1$ the spectrum is essentially that of a laser whose frequency is slowly scanned from $\omega-\Delta\omega$ to $\omega+\Delta\omega$, as one would expect.

After performing these calculations, students can generate spectra in the laboratory by applying an rf modulation to the laser injection current and by using the scanning confocal cavity described in the previous section. Typical results are

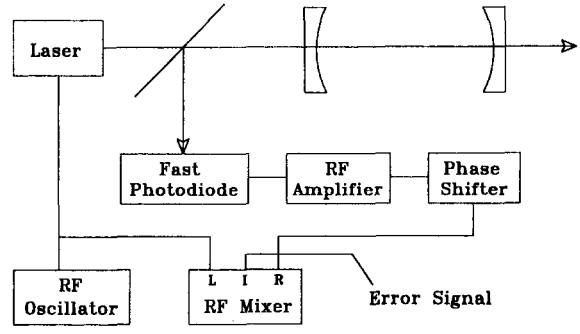

Fig. 9. Optical and electronics layout for the Pound–Drever experiment. Part of the light reflecting off the Fabry–Perot cavity falls on a fast photodiode, and the high-frequency component of the photocurrent is amplified and phase-shifted (using a length of BNC cable) before being mixed with the local oscillator to form an error signal.

shown in Fig. 8. Although the laboratory spectra reproduce the calculated spectra fairly well, there is a marked asymmetry in the lab spectra, which is best seen in Fig. 8(c). This appears as a result of amplitude modulation of the diode laser, which was neglected in the pure-FM calculation.

IV. THE POUND–DREVER METHOD

In many precision optical experiments it is desirable to have a laser with a well-defined frequency. For example, many atomic physics experiments require lasers with frequencies fixed on or near atomic resonance lines. For tunable lasers it is therefore necessary to have a means of controlling the laser's frequency, and of "locking" it at a desired value. This experiment is an introduction to the Pound–Drever method[14] of laser frequency stabilization. The method uses techniques of optical heterodyne spectroscopy and radio-frequency electronics that are in widespread use in modern research laboratories. Although these techniques can be used to reduce laser linewidths to sub-Hz levels,[13] we will limit ourselves here to laser frequency (and not phase) stabilization only.

There are a number of techniques that can be used to lock a laser's frequency. One of the simplest is the "side-locking" method. One starts with frequency-selective optical element which produces a voltage signal as a function of laser frequency $V(\omega)$. If one wishes to lock the laser frequency at ω_0, and $dV/d\omega(\omega_0)\neq 0$, then one subtracts a reference voltage to make an error signal $\epsilon(\omega)=V(\omega)-V(\omega_0)$. This error signal then serves as input to a feedback loop which adjusts the laser's frequency to make $\epsilon=0$. The side-locking method is useful if one wishes to lock to the side of a peaked resonance feature.

Often one would like to lock to the *peak* of a resonance feature, such as at the peak in cavity transmission in Fig. 6, which gives a voltage signal with $dV/d\omega(\omega_0)=0$. The side-locking method would not work here, since a nonzero error signal alone is insufficient to determine whether the laser frequency should be increased or decreased. One technique that does work in this circumstance is to dither the laser frequency slowly at a frequency Ω, producing a voltage signal $V(t)=V(\omega(t))\approx V[\omega_{\text{center}}+\Delta\omega\cos(\Omega t)]$. As in the previous section, with $\beta=\Delta\omega/\Omega \gg 1$, the voltage signal $V(t)$ behaves as if the laser frequency were slowly oscillating back and forth. A lock-in amplifier with reference frequency Ω produces an error signal $\epsilon(\omega)$, which is the Fourier compo-

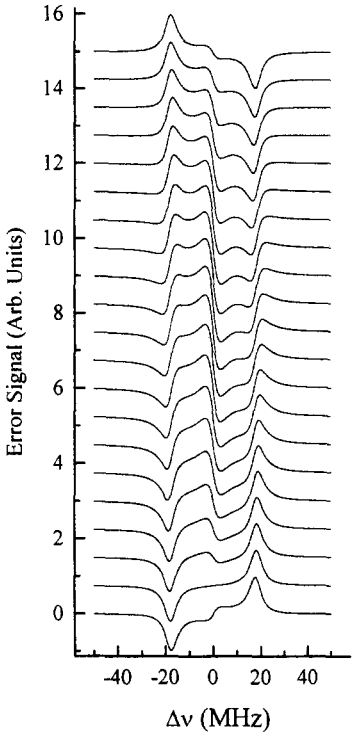

Fig. 10. Calculated error signal as a function of laser frequency, for various phase shifts Δ. The rf modulation frequency was taken to be $\Omega/2\pi=18$ MHz, and the cavity reflectivity was set at $R=0.95$. The phase shift of the bottom plot is zero and increases upward in steps of $\pi/20$; the different plots are offset for ease of viewing.

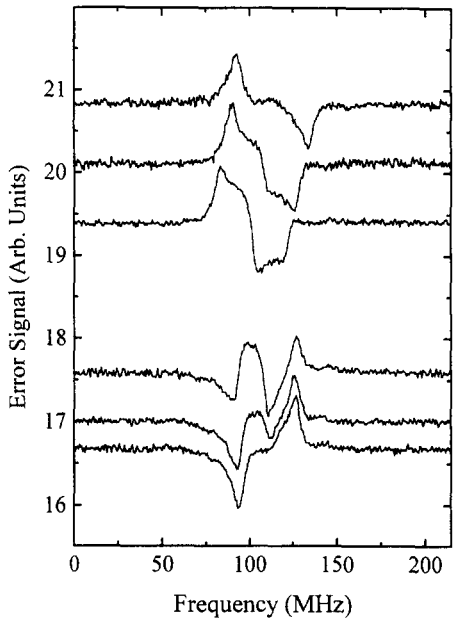

Fig. 11. Measured Pound–Drever error signals, as described in the text. Here, the offset of each plotted line is equal to the modulation frequency in MHz. Changing the modulation frequency not only changes the sideband spacing but also changes the phase factor Δ. Note that a variety of error signal forms can be produced, which correspond to those in Fig. 10. Again, one sees an asymmetry originating from the residual amplitude modulation of the laser light.

nent of $V(t)$ at frequency Ω. It is easily seen that on resonance we have $\epsilon(\omega_0)=0$, and for small dither amplitudes $d\epsilon/d\omega(\omega_0)\neq 0$; thus this error signal can be used in a feedback loop to lock the laser frequency at ω_0.

The main disadvantage of this simple dither-locking method is that the servo bandwidth is limited to a frequency less than the dither frequency Ω, which, in turn, must be much less than the frequency scan $\Delta\omega$, and thus less than the linewidth of the resonance feature on which one wishes to lock. For a resonance feature a few MHz wide, typical of atomic transitions, the servo bandwidth with this technique is then limited to the point that acoustic noise on the laser cannot be adequately removed.

The Pound–Drever method extends the dither-locking concept into the regime where $\beta\ll 1$, considerably improving the available servo bandwidth. With a well-designed feedback network, the Pound–Drever method can be employed to greatly reduce the sub-MHz acoustic noise on a laser.

In this lab we demonstrate the Pound–Drever method by using a servomechanism to lock a Fabry–Perot cavity peak and laser to each other. One can lock the laser to the cavity or lock the cavity to the laser, but, in practice, we have found it easier to do the latter. Although for best results the cavity can be isolated from temperature changes and vibrations, our experience indicates that an optical breadboard provides sufficient stability. Since the cavity PZT has a limited frequency response, the servo is not very effective at removing high-frequency acoustic noise; nevertheless, in practice, the lock is robust, and the apparatus is fairly easy to assemble.

The basic layout we use for the Pound–Drever method is shown in Fig. 9. FM sidebands are added to the laser, producing two weak sidebands at frequencies $\omega\pm\Omega$ around the laser's central carrier frequency at ω. The modulation frequency Ω is chosen to be slightly greater than the width of the cavity transmission peaks. The modulated laser beam is directed onto the cavity, where part of the beam is transmitted and part is reflected. The reflected part encounters a 50:50 beamsplitter which directs half the reflected light onto a fast photodiode. The photodiode output is amplified, phase shifted, mixed with the rf oscillator, and low-pass filtered to produce an error signal.

If the laser and the cavity are in resonance, the carrier is mostly transmitted while the sidebands are mostly reflected. These fields all have fixed phase relationships, and their sum produces a photocurrent containing no component at the modulation frequency. If the laser and the cavity drift out of resonance, a photocurrent signal appears at the modulation frequency Ω. This signal is pulled out by the mixer and becomes the error signal. The error signal can be calculated with the following analysis, adapted from Bjorklund *et al.*[15] The reflection amplitude from an etalon is given by[7]

$$E_r=\frac{(1-e^{i\delta})\sqrt{R}}{1-Re^{i\delta}}E_i\equiv A(\delta,R)E_i,$$

where R is the mirror reflectivity and $\delta=2\pi\Delta\omega/\Delta\omega_{\mathrm{FSR}}$. For $\beta\ll 1$ we can write the input as a carrier and two weak sidebands

$$E_i=E_0\{-Me^{i(\omega-\Omega)t}+e^{i\omega t}+Me^{i(\omega+\Omega)t}\},$$

which gives

$$E_r=E_0e^{i\omega t}\{-MA_-e^{-i\Omega t}+A_0+MA_+e^{i\Omega t}\},$$

where $A_0=A(2\pi\Delta\omega/\Delta\omega_{\mathrm{FSR}},R)$ and $A_\pm=A(2\pi(\Delta\omega\pm\Omega)/\Delta\omega_{\mathrm{FSR}},R)$. The photodiode signal is then $I_{\mathrm{phot}}\propto|E_r|^2$, which is a real function containing dc terms and terms proportional

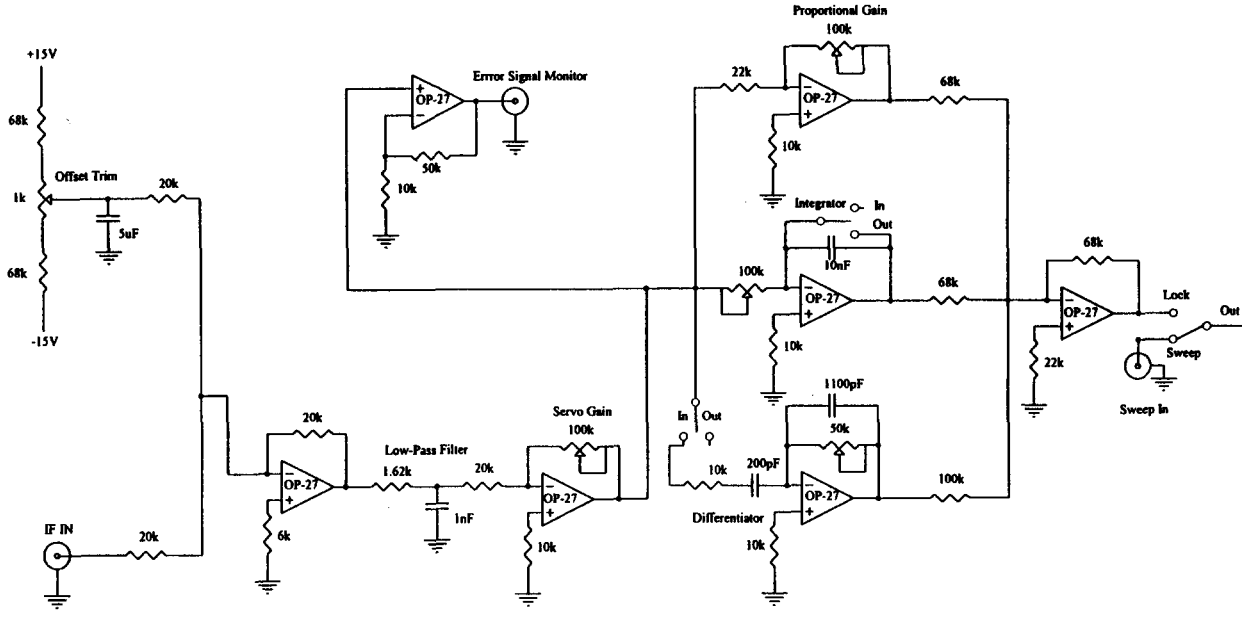

Fig. 12. Schematic diagram of the "lock box" used in the Pound–Drever experiment to lock the cavity resonance frequency to the laser frequency. Note that removable proportional, integral, and differential feedback stages are present in the circuit, each with its own adjustable gain.

to cos Ωt and sin Ωt. The effect of the mixer is essentially to multiply the photodiode signal by $\exp(i\Omega t+\Delta)$ and take the real part, where Δ is a phase factor depending on the relative phase of the photodiode and local oscillator signals at the mixer. Low-pass filtering gives the error signal

$$I_{\text{error}} \propto \text{Re}\{e^{i\Delta}(A_0^* A_+ - A_0 A_-^*)\},$$

shown in Fig. 10 for a variety of phase factors.

After calculating expected error signals, the first student exercise in this lab is to set up the equipment to generate an error signal in the lab. The optical layout (see Fig. 9) is relatively simple, and it uses the Fabry–Perot cavity which has already been set to its confocal length. The required rf amplifiers and fast photodiode can be purchased from standard rf electronics suppliers, but one can realize considerable savings by constructing them oneself from more basic components. For the photodetection, it is essential to choose a photodiode with a bandwidth greater than the modulation frequency. We use an EG & G HFD-1060 photodiode, which includes an amplifier built into the same package. The response falls off above a few hundred MHz, which is more than sufficient for our experiments. The NE5205AN is an inexpensive rf amplifier chip, giving about 17 dB of gain, and we usually use at least two stages for this experiment.

For the construction of the rf circuitry it is essential that proper construction techniques be used. The circuits must be laid out on double-sided copper-clad printed-circuit boards. To improve the ground plane we also connect both copper sides of the board to each other using copper foil soldered along all edges of the board. Furthermore, all component leads should be kept as short as possible, and rf signals should be led to and from the circuit by pieces of shielded coaxial cable.

For the mixer (see Fig. 9) we use a Mini-Circuits ZAD-1, which functions best with a local oscillator power of 7 dBm. This rf power level makes the modulation index (β) of our laser too large, so we typically insert a 10- or 20 dB attenuator between the rf source and the laser current controller. Our phase shifter is nothing more than a length of BNC cable. The phase factor can also be shifted by changing the rf modulation frequency.

Figure 11 shows some error signals generated with this setup, after low-pass filtering to reduce the frequency-doubled components of the signal coming from the mixer. The measured error signals are similar to the calculated ones (see Fig. 10), again with an asymmetry arising from the residual amplitude modulation of the laser.

The final exercise in this lab is to use the error signal in a servo system to lock the laser and cavity frequencies. Once locked, the cavity transmission stays at its peak value, which can be monitored by a separate (slow) photodiode. We use the "lock-box" shown in Fig. 12 for this purpose, which includes removable proportional, integral, and differential gain stages. Once the lock is established, the students can examine the behavior of the lock with and without the various feedback stages.

ACKNOWLEDGMENTS

This work was supported in part by the National Science Foundation under the Instrumentation and Laboratory Improvement program, and by the California Institute of Technology. We thank Phil Willems for many useful discussions, and for his efforts in the design of several electronics components used in this lab.

[a]E-mail: kgl@sundog.caltech.edu

[1]K. G. Libbrecht, R. A. Boyd, P. A. Willems, T. L. Gustavson, and D. K. Kim, "Teaching physics with 670-nm diode lasers—Construction of stabilized lasers and lithium cells," Am. J. Phys. **63**, 729–737 (1995).

[2]We have found ways to increase the number of students that can productively use one setup by: (1) having students work in pairs; and (2) scheduling pairs of students to come in at different times to use the same apparatus. Our experience is that at least three pairs of students can use the same setup by arranging them to come at different times during a one-week experiment. However having separate setups for each pair of students is desirable.

[3]D. M. Kane, "The use of the nearly confocal interferometer for the study of transverse modes of a cavity," Am. J. Phys. **59**, 235–239 (1991).
[4]A. Poloeanu and I. Popescu, "Some simple experimental studies using a passive cavity coupled to a HeNe laser cavity for practice in a quantum electronics laboratory," Am. J. Phys. **57**, 646–654 (1989).
[5]J. C. Amato, R. E. Williams, and H. Helm, "An inexpensive, easy to build Fabry–Perot interferometer and its use in the introductory laboratory," Am. J. Phys. **59**, 992–994 (1991).
[6]N. Whitlatch, "Spectrum analysis of optical resonators," Am. J. Phys. **58**, 556–566 (1990).
[7]A. Yariv, *Optical Electronics* (Holt, Rinehart and Winston, New York, 1991), 4th ed.
[8]Our source was Virgo Optics, which provided the mirror substrates as well as the coatings at a cost of $1900.00 for 20 pieces. A number of other vendors, such as Lightning Optical, can provide the same service.
[9]Thor Labs part No. RA90, or equivalent.
[10]Thor Labs part No. AD1.
[11]Hewlett–Packard model HP54600A.
[12]K. G. Libbrecht and J. L. Hall, "A low-noise high-speed diode laser current controller," Rev. Sci. Instrum. **64**, 2133–2135 (1993).
[13]J. L. Hall and M. Zhu, "An Introduction to Phase-Stable Optical Sources," *Proceedings of the International School of Physics—Enrico Fermi*, 1992, edited by E. Arimondo, W. D. Phillips, and F. Strumia (North-Holland, Amsterdam, 1992).
[14]R. W. P. Drever *et al.* "Laser phase and frequency stabilization using an optical resonator," Appl. Phys. B **31**, 97–105 (1983).
[15]G. C. Bjorklund *et al.*, "Frequency-modulation (FM) spectroscopy—theory of line shapes and signal-to-noise analysis," Appl. Phys. B **31**, 145–152 (1983).

Laser spectroscopy of the cesium dimer as a physics laboratory experiment

Mark Terrell and Mark F. Masters
Indiana-Purdue University at Fort Wayne, Fort Wayne, Indiana 46805

(Received 30 October 1995; accepted 13 March 1996)

Laser spectroscopy of the cesium dimer is presented for use in an undergraduate laboratory. The experimental apparatus consists of near 780-nm diode lasers, a glass cesium cell, a simple oven, and a monochromator. The experiment can be assembled quickly and at low cost. In the course of this experiment students can observe vibrational structure in molecular emission and learn about potential energy curves and Franck–Condon factors. The first vibrational constant of the $X^1\Sigma_g^+$ ground state is measured to be 42.7 ± 1.6 cm^{-1}. © *1996 American Association of Physics Teachers.*

I. INTRODUCTION

Atomic spectroscopy, both Doppler-broadened and Doppler-free, of the rubidium hyperfine structure has become very popular as a modern physics experiment because of the availability of rubidium cells and low-cost diode laser systems.[1–3] Diode lasers provide a narrow bandwidth (~10 MHz), single-mode, stable, tunable laser source near 780 nm at a relatively low cost. These same properties can also be used for other spectroscopy experiments such as the spectroscopy of the cesium dimer. Because of the density of rovibrational (rotational–vibrational) transitions in dimers, this experiment is able to use any nominally 780-nm diode laser. The spectrally resolved fluorescence spectrum can be analyzed to determine the first two vibrational constants of the ground state and even the first vibrational constant of the excited state.

We chose cesium because glass cesium cells can be obtained at relatively low cost,[4] a high density of cesium vapor and cesium dimers can be formed at fairly low temperatures, and there are some molecular transitions near 780 nm. Additionally, the lowest three singlet states of the cesium dimer have been accurately mapped.[5–7] It is these states which we are probing with the diode laser.

Using diode lasers near 780 nm (775–788 nm), we are able to optically excite Cs_2 from various rovibrational levels in the ground state ($X^1\Sigma_g^+$) to vibrational levels of an electronically excited state. Light with a wavelength of 780 nm will excite the molecules to either high lying vibrational levels of the $A^1\Sigma_u^+$ state or low lying vibrational levels of the $B^1\Pi_u$ state (see Fig. 1). We observe fluorescence from the excited vibrational levels back to various vibrational levels of the ground state. This fluorescence is used to determine the first vibrational constant of the cesium ground state and to determine which excited state we are probing.

II. EXPERIMENT

The experimental setup is shown in Fig. 2. The diode laser current and temperature controllers are of the same design as described by Brandenberger[3] but use a 5-mW Sharp LTO 22M, 780-nm diode laser. The laser beam enters an oven which contains the glass vapor cell. Fluorescence perpendicular to the laser beam is collected with a lens and focused on a monochromator or spectrograph entrance slit. The monochromator is a 1/4-m Ebert design with a 600-g/mm 1-μm blaze grating equipped with an uncooled near S-1 response photomultiplier tube [R406 (S-1 response provides sensitivity from 400–1100 nm with peak sensitivity at 730 nm)]. The signals were amplified by an electrometer, digi-

